UNIVERSITY OF WEST BOHEMIA

Applied and Computational Mechanics 1 (2007) 677 - 684

Applied and Computational Mechanics

Buoyancy driven turbulent flow and experimental validation at the VeMix test facility

R. Vaibar[a,*], M. J. Da Silva[a], T. Sühnel[a]

[a] *Forschungszentrum Dresden Rossendorf, Bautzner Landstrae 128, 01328 Dresden - Germany*

Received 11 September 2007; received in revised form 12 October 2007

Abstract

Buoyancy driven flow is often found in many engineering application such as the mixing process of fluids, which have different densities. The aim of this study is to simulate mixing of borated and unborated water, an issue which is relevant to the analysis of the safety of nuclear reactors. The degree of mixing of weakly and highly borated coolant is a critical issue with respect to reactivity of the reactor core. Therefore, a combined numerical and experimental study of buoyant mixing processes has been performed. As nuclear reactor geometries are complex, a vertical mixing (VeMix) test facility was used to validate the numerical models used with optical and surface wire mesh measurements. Good agreement was found between the physicality of the flow phenomena of the observed experiments and numerical calculations. Fourier analysis of the vortical oscillations in both the experiments and simulations also show good agreement for several flow conditions.

Keywords: buoyancy, turbulence modelling, wire-mesh sensor

1. Introduction

Buoyancy driven flow is often found in many engineering application such as mixing process of fluids with different density. The aim of our study is to simulate mixing processes that are relevant to the analysis of the safety of nuclear reactors. The boron dilution problem is one such safety issue that requires analysis. Borated water is used to moderate the nuclear reactions occuring in the reactor core. However, in certain situations, additional borated water in the form of boric acid is added to the core, which may have a different temperature. Both the boron concentration and the temperature will affect the density difference of the fluids being mixed and therefore affect the mixing processes that occur in such situations. Thus, the degree of mixing of low and high borated coolant is a critical issue with respect to reactivity insertion into the reactor core. A very simple vertical test facility was chosen for validation of numerical models of the mixing process, as nuclear reactor geometries are complex leading to the mixing processes that are not widely understood and the small influence of the buoyancy. A new source term, which consists of a sum of the component turbulent density fluxes, is defined for the turbulence model and in this case it is based on the definition turbulent kinetic energy.

2. Theoretical model

Buoyancy is driven by variations in density, which can arise, as in this case, from *multicomponent flows* through the variation of the mass fraction caused by local mixing.

*Corresponding author. Tel.: +49 351 260 3408, e-mail: r.vaibar@fzd.de.

For buoyancy calculations, a source term is added to the momentum equations as follows:

$$S_{M,buoy} = (\rho - \rho_{ref})\, g,$$

ρ the evaluated mixture density calculated directly using the Full Buoyancy model from the concentration of each component and the density for each component,

$\rho_{ref} = \frac{1}{N}\sum_{i=1}^{N} \rho_i$ the relative density calculated as an average density of all N components in mixture,

g the acceleration due to gravity.

2.1. Buoyancy induced turbulence

The influence of buoyancy on the turbulence model could be added via source term in equation for turbulent kinetic energy k. A typical example of the models that can characterise the turbulent kinetic energy are "two-equations" family of turbulence models i.e. $k-\epsilon$, $k-\omega$ and their combinations such as Shear Stress Transport (SST). The modification of SST model of the form below is the focus of this study:

$$\begin{aligned}
\frac{D\rho k}{Dt} &= \nabla\left(\mu + \frac{\mu_t}{\sigma_k}\right)\nabla k + P_k + P_b - \rho\epsilon, \\
\frac{D\rho\omega}{Dt} &= \nabla\left(\mu + \frac{\mu_t}{\sigma_\omega}\right)\nabla\omega + (1-F_1)2\rho\frac{1}{\sigma_\omega}\nabla k\nabla\omega + C_{1\omega}\frac{\omega}{k}\left(P_k + C_{2\omega}P_b\right) - \beta\rho\omega^2,
\end{aligned}$$

$\frac{D\rho k}{Dt} = \frac{\partial \rho k}{\partial t} + (\nabla U.\rho k)$ material derivative of variables ρ, k, U fluid velocity,

μ molecular viscosity,

$P_k = -\rho\overline{u_i u_j}\frac{\partial u_j}{\partial x_i} = \mu_T\sqrt{2S_{ij}S_{ij}}$ production term due to viscous forces,

$P_b = -\sum_{i=1}^{3} g_i\overline{\rho u_i}$ general form of production due to buoyancy forces,

$P_b = -g\frac{\mu_T}{\rho Pr_t}\triangle\rho$ standard turbulent buoyancy model in ANSYS CFX,

$\omega = \frac{\epsilon}{C_\mu k}$ turbulent frequency,

F_1 blending function limiting ω to the boundary layer [1],

$\mu_t = \rho\frac{a_1 k}{\max(a_1\omega, SF_2)}$ turbulent viscosity, F_2 blending function ,

S invariant measure of the strain rate,

$C_\mu, \sigma_k, \sigma_\omega, C_{1\omega}, C_{2\omega}, \alpha, \beta$ constants of SST model [1].

P_b describes the influence of buoyancy to the turbulent model [3]. This term could be modeled by solving the proper transport equations for components of Reynolds-averaged turbulent density fluxes, $\overline{\rho u_i}$, which have the form:

$$\begin{aligned}
\frac{D\overline{\rho u_i}}{Dt} = \underbrace{\frac{\partial}{\partial x_j}\left(\underbrace{\alpha\overline{\frac{\partial\rho}{\partial x_k}u_i} + \nu\rho\overline{\frac{\partial u_i}{\partial u_k}}}_{D^{\nu}_{\rho i}} \underbrace{-\overline{\rho u_i u_k}}_{D^{t}_{\rho i}}\right)}_{D_{\rho i}} \underbrace{-\overline{\frac{\partial p}{\partial x_i}}}_{\Pi_{\rho i}} - \underbrace{(\alpha+\nu)\overline{\frac{\partial\rho}{\partial x_k}\frac{\partial u_i}{\partial x_k}}}_{\epsilon_{\rho i}} - \\
\underbrace{\underbrace{-\overline{u_i u_k}\frac{\partial\rho}{\partial x_k}}_{P^{\rho}_{\rho i}} \underbrace{-\overline{\rho u_k}\frac{\partial U_i}{\partial x_k}}_{P^{U}_{\rho i}} \underbrace{-g_i\overline{\rho^2}}_{G^{th}_{\rho i}}}_{Production},
\end{aligned} \tag{1}$$

$D^{\nu}_{\rho i}$ molecular diffusion,
$D^{t}_{\rho i}$ turbulent diffusion,
$\Pi_{\rho i}$ pressure scrambling effect,
$\epsilon_{\rho i}$ molecular destruction term,
$P^{\rho}_{\rho i}$ production term due to mean density gradient,
$P^{U}_{\rho i}$ production term due to mean velocity gradient,
$G^{th}_{\rho i}$ buoyancy due to density variance.

Equation for density variance - $\overline{\rho^2}$ is:

$$\frac{D\overline{\rho^2}}{Dt} = \underbrace{\frac{\partial}{\partial x_k}\left(\underbrace{\alpha\frac{\partial\overline{\rho^2}}{\partial x_k}}_{D^{\nu}_{\rho^2}}\underbrace{-\overline{\rho^2 u_k}}_{D^{t}_{\rho^2}}\right)}_{D_{\rho^2}}\underbrace{-2\overline{\rho u_k}\frac{\partial\rho}{\partial x_k}}_{P_{\rho^2}} - \underbrace{2\alpha\overline{\frac{\partial\rho}{\partial x_k}\frac{\partial\rho}{\partial x_k}}}_{\epsilon_{\rho^2}}, \tag{2}$$

D_{ρ^2} the total diffusion of density scale, ρ^2,
$D^{\nu}_{\rho^2}$ the molecular diffusion of density scale, ρ^2,
$D^{t}_{\rho^2}$ the turbulent diffusion of density scale, ρ^2,
P_{ρ^2} production term due to mean density gradient,
ϵ_{ρ^2} the molecular destruction term.

The presented model was implemented into the ANSYS CFX code by using pre-defined additional variables, according to the balance equation:

$$\frac{\partial\Phi}{\partial t} + \nabla(U\Phi) = \nabla\left(\left(\rho D_{\Phi} + \frac{\mu_t}{Sc_t}\right)\nabla\left(\frac{\Phi}{\rho}\right)\right) + S_{\Phi},$$

ρ the mixture density, mass per unit volume,
Φ the conserved quantity per unit volume, or concentration,
$\frac{\Phi}{\rho}$ the conserved quantity per unit mass,
S_{Φ} the volumetric source term, with units of conserved quantity per unit volume per unit time,
D_{Φ} the kinematic diffusivity for the scalar,
μ_t the turbulence viscosity, with Sc_t the turbulence Schmidt number.

For full implementation of presented model, four equations were applied, three of which were used for description of the three components of turbulent density fluxes $\overline{\rho u_i}$. Where the fourth equation was an equation for density variance $\overline{\rho^2}$.
If the transport effect in equations (1) is neglected, the Algebraic Flux Model for turbulent density fluxes is obtained:

$$\overline{\rho u_i} = -C^{\rho}\frac{k}{\epsilon}\left(\overline{u_i u_j}\frac{\partial\rho}{\partial x_j} + \xi\overline{\rho u_j}\frac{\partial U_i}{\partial x_j} + \eta\beta g_i\overline{\rho^2} + \epsilon_{\rho_i}\right). \tag{3}$$

From this assumption several simplifications can be defined in which more and more of the terms on the right hand side of equation (3) are neglected. Then by considering only the first term of equation (3) gives:

$$\overline{\rho u_i} = -C^{\rho}\frac{k}{\epsilon}\overline{u_i u_j}\frac{\partial\rho}{\partial x_j}. \tag{4}$$

If the sum over all turbulent density fluxes is taken then the isotropic source term of the standard model used in ANSYS CFX is obtained, as the simplest borderline case of our model:

$$P_b = g \sum_{i=1}^{3} \overline{\rho u_i} = -g \frac{\mu_T}{\rho Pr_t} \triangle \rho,$$

which is often used in standard CFD [1] codes for modelling of buoyancy influence to the turbulence model.

3. VeMix experimental vessel

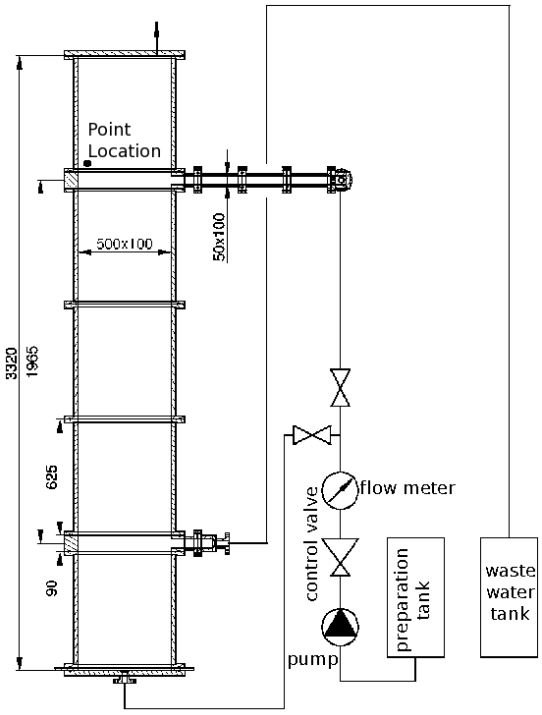

For the validation of the model, which was implemented into ANSYS CFX, an experimental facility called **VeMix** - **Ve**rtical **Mix**ing channel was built. The VeMix test facility has a simple geometry and it was setup to ensure that the gravity force acts along the significant length scale, the height. Five plexiglas units were constructed to allow the observation of the flow patterns formed and to also allow the use of laser based measurement techniques such as LDA and PIV.

In the *preparation tank*, the water is mixed to the required density by adding saccharose and the required conductivity by adding salt. This tank is connected to the bottom input and to the upper inlet nozzle of the vertical section. The output nozzle is connected to the *waste water tank*.

Fig. 1. VeMix scheme.

Experiment proceduce has the following steps:

1 modify the conductivity of the water in the *preparation tank* by adding salt so that ($\kappa = 60$ μS cm^{-1})
2 then fill almost the whole of the VeMix test facility with the water from the *preparation tank* via either inlet
3 modify the density and conductivity of the water in the *preparation tank* by adding saccharose and salt so that there is a 2% density difference and ($\kappa = 200$ μS cm^{-1})
4 fill up the vertical section up to 2.12 m from bottom. The bottom unit, which includes the surface wire mesh sensor should be covered by this water. The flow pattern formed is dependent on the level of the water with modified density filling of the VeMix vessel
5 set the desired flowrate via the flow meter before starting to pump the water with modified density from the tank to the VeMix though the upper inlet nozzle.
6 initially, normal water from the pipeline system is fed to the VeMix vessel, creating a jet of normal water entering the vessel, which forms a layer

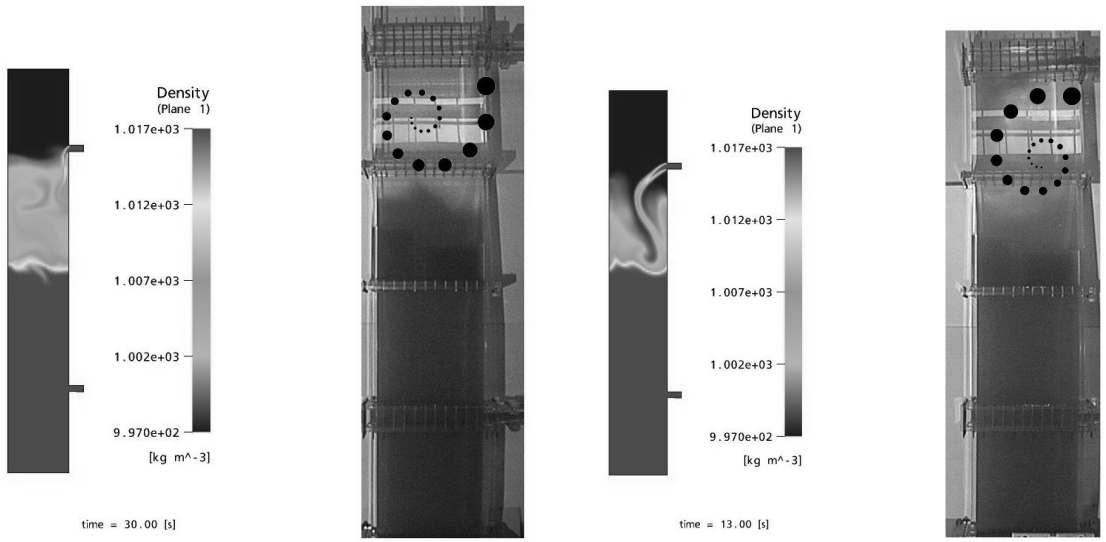

(a) Falling down regime $flowrate = 0.4\,\mathrm{l\,s^{-1}}$, $Ri = 2.12$.

(b) Horizontal jet regime $flowrate = 0.7$ l s^{-1}, $Ri = 0.69$.

Fig. 2. Flow regime during the flow condition $\Delta\rho = 2\%$, $H_{fill} = 1.8$ m and given flowrate.

7 after a short period of time, defined by the amount of normal water in the pipelines and flowrate used, the density modified water enters the vessel and mixing between the modified and normal waters begins

8 the conductivity measured by the surface wire mesh sensor corresponds to the fraction of normal water and density modified waters

9 the water leaving via the output nozzle is then fed to the waste water tank

4. Results

The different the flow conditions were defined to give typical flow patterns. This flow behaviour can be characterised by an internal Richardson number of form

$$Ri(\triangle\rho, fl, H_{fill}) = \frac{g * L^2 * \triangle\rho}{\rho * v^2}, \quad L = H_{input} - H_{fill}, \tag{5}$$

where L is the characteristic length, $H_{input} = 2.63$ m distance of bottom part of the inlet nozzle from bottom of VeMix vessel, H_{fill} distance of interface between the liquid from bottom of VeMix vessel, $\triangle\rho$ density difference, $\rho = 997$ kg m^{-3} density of water, $v = \frac{flowrate}{Surface}$ characteristic flow velocity describing the movement of interface between the liquids, fl input flowrate, $Surface = 0.5 * 0.1$ m^2 surface of VeMix vessel.

The Froude number has been widely used to characterise buoyant mixing; however, the Froude number is inversely dependent on the internal Richardson number, $Fr = \frac{1}{\sqrt{iRi}}$. As the Richardson number has a greater sensitivity to the characteristic flow patterns at the transition of the flow regimes. Thus, the internal Richardson number is used to qualitatively characterise the flow regimes observed in this study:

falling down regime of flow patterns $Ri > 2$ are shown in Figure 2a, for both the experiment and the simulation at time $t = 30$ s. Figure 2a clearly shows that the gravity force acts along the vertical axis and is significantly stronger than momentum forces. The jet drops down near the wall below the inlet nozzle.

horizontal jet regime of flow patterns $Ri < 1$ shown on Figure 2b, for both the experiment and simulation at $t = 13$ s. In this case, the momentum force driven by the input flowrate is stronger than the gravity force, which results in the formation of a horizontal jet. The horizontal jet influences the transient mixing behaviour, as oscillation waves are formed on interface between the heavier, density modified water (darker fluid) and the normal water (transparent fluid).

4.1. Analysis of oscillation frequencies

The frequencies of the oscillation waves in the layer between the heavier, density modified and normal waters above the horizontal jet were found via a Fourier analysis of the video signal. The Fourier analysis characterised the 3 components of video signal (RGB) from the digital camera signal and from the pictures created in CFX5Post. A point location above the inlet nozzle was chosen where the oscillation between the darker and transparent fluids occurs in experimental case and between the changing the color in simulation case. The selected location was at $X = 0.1$ m, $Y = 2.7$ m. The significant frequencies found in both Fourier power spectra corresponds to the frequency of oscillation wave, but the turbulent energy in the numerical case is much lower. A possible explanation of the discrepancy in the magnitudes of the spectra is that at the selected point in the experiment, the data stored is an integral over the depth of the section.
Figure 3a shows the base time series and the corresponding Fourier power spectra for the analysis of the simulated case on the left and the video data obtained from the experiment on the right. Figure 3b shows the dependency of osclilation frequencies on the flowrate, where other paramaters were fixed at $\Delta\rho = 0.02$ and $H_{fill} = 2$ m. Good agreement between the experimental and simulated cases can be observed in Figure 3b.

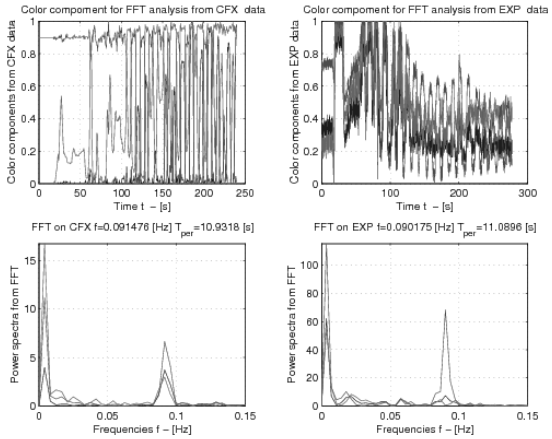

(a) Fourier analysis for case $\Delta\rho = 2\%, H_{fill} = 2m, fl = 0.45\,\mathrm{l\,s^{-1}}$.

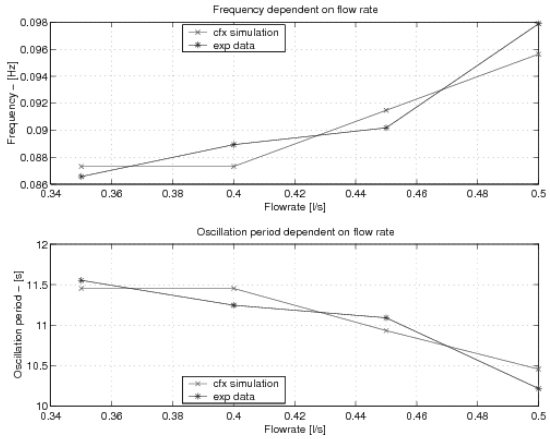

(b) Oscilation frequency and periodic time profile with respect to the flowrate.

Fig. 3. Fourier analysis of video data signal and oscilation frequencies.

4.2. Surface wire mesh sensor [2]

The array sensor used here was manufactured using standard printed-circuit board fabrication technology and has 4096 interdigital sensing structures, which are multiplexed in a matrix with 64 transmitter (rows) and 64 receiver electrodes (column). Figure 4 presents the surface sensor and in detail depicts the structure of the sensors. The *so-called* spatial wavelength is defined as the distance between the centerlines of neighboring electrodes of the same type (e.g.

driving or sensing electrodes) and has the value of 2.6 mm for the sensor used here. The depth of penetration of the electric field generated by an interdigital sensor into the material is proportional to the spatial wavelength [4]. Furthermore, the electrodes are gold plated to reduce electrochemical effects during the conductivity measurement. The sensor board was designed to fit to an experimental flow channel. The size of the whole sensor is 620mm x 500 mm. Four connectors on the back side of the sensor (not shown in fig. 4) allow the sensor to be connected to recording devices. The voltage values measured by the surface sensor are proportional to the electrical current flowing from the transmitter electrode to the receiver electrode. This current basically depends on two parameters; the electrical conductivity κ of the liquid and on liquid wetting level of a sensing structure. The dependency of the application these parameters can be explored for the generation of information of how the fluid is distributed over the sensor. Since the system has only one measurement for two unknowns, in order to generate an unambiguous output, one of the parameters must be known or kept constant during the experiments. Therefore, two different conditions can be investigated. In the case where the wetting level is constant (i.e when the sensing structures are always covered by liquid) the use of conductivity tracers can be used to evaluate the flow in the channel. The second possibility is for the case when a liquid with constant conductivity is used and only its distribution over the sensor is of interest. For instance, the presence of gas bubbles on the surface can be detected due the fact the bubbles will change the wetting level of a sensing structure.

The most interesting location in the VeMix vessel was found to be just below the inlet nozzle. Therefore, the sensor was placed here in order to study the transition behaviour of jet between the vertical and horizontal regimes. The comparison between the simulated data and the data obtained from surface wire mesh sensor is depicted in Figure 5. A grid of data points was obtained from the data measured by surface wire mesh sensor. This grid was imported into CFX5Post to generate a field to which experimental and numerical data could be mapped. The contour plots of the experimental and simulated data derived from this field are presented in Figure 5 at time $t = 28.1$s for the case $\Delta\rho = 0.02$, $flowrate = 0.35$ l s^{-1}, $H_{fill} = 2.12$ m. This gave an internal Richardson number of 1.06. For all the contour plots, the development of the horizontal jet is clearly seen, as can be expected for a flow at such a internal Richardson number, which lies close to the lower limit of the transition regime between horizontal and vertical jet flow $iRi \in (1, 2)$. However, the difference between modified buoyancy term and the standard term was small.

5. Conclusion

A new source term that was defined via the sum of components of turbulent density fluxes was implemented into the ANSYS CFX code. Validation experiments were performed in the VeMix test facility, which show typical vertical and horizontal flow pattern under different flow regimes. Comparisons of the experimental results with corresponding simulations show similar flow patterns and periodic behaviour. The data from the surface wire mesh sensor was used for the validation against the data from the simulation. The influence of the buoyancy on the turbulence model was shown to be small through comparison between the implemented and standard buoyancy models.

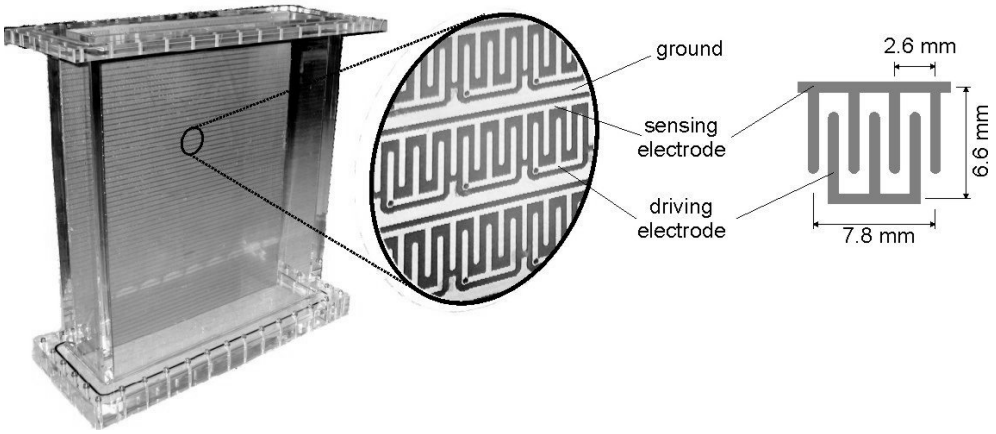

Fig. 4. Printed circuit board surface sensor containing 64 x 64 interdigital sensing structures fitted to an experimental flow channel. The size of each sensing structure is 7.8 mm x 6.6 mm and the size of the whole sensor is 620 mm x 500 mm.

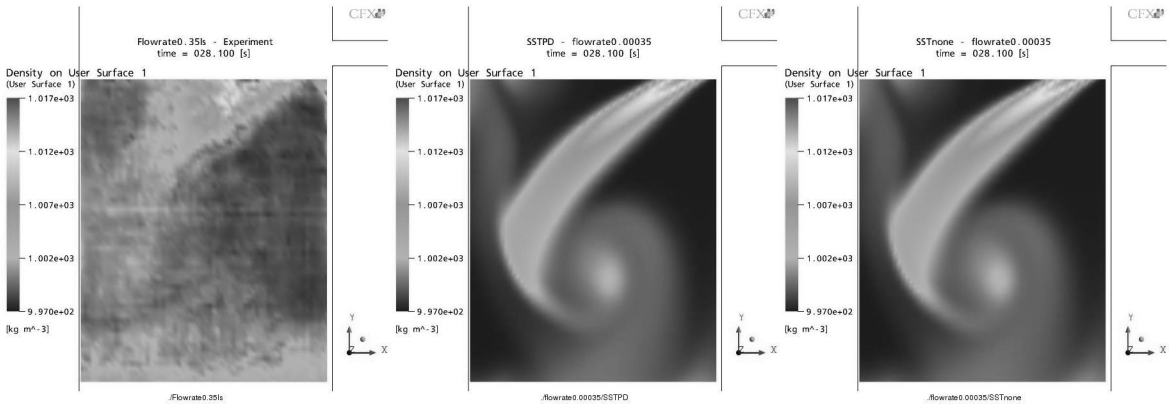

Fig. 5. Contour plots of the horizontal jet. Left - data obtained by the surface wire mesh sensor, Centre - Simulation performed with only the SST model, Right- Simulation performed with the modified buoyancy driven turbulence term applied to the SST model, at time T=28.1 [s].

Acknowledgements

The project is funded by the German Federal Ministry of Economy and Labour, grant No. 150 1287. We would also like to thank Tobias Sühnel for constructing the VeMix facility and performing the experiments discussed here.

References

[1] ANSYS Europe Ltd., CFX 10.0 Documentation, Turbulence and near-wall modelling, 2005.
[2] M. J. Da Silva, T. Sühnel, E. Schleicher, D. Lucas, R. Vaibar, U. Hampel, Planar array sensor for high-speed component distribution imaging in fluid flow applications, Sensors 2007.
[3] K. Hanjalić, One-point closure models for buoyancy driven turbulent flows, Fluid Mechanics 34, 2002, 321-347.
[4] X.B. Li, S.D. Larson, A.S. Zyuzin, A.V. Mamishev, Design Principles for Multichannel Fringing Electric Field Sensors, IEEE Sensors 2006, 6, 434-440.